Development of Ductile T-Joint in Box-Column by Electroslag Welding

KUAN-HAO LIN, HSUN-JUNG CHEN, MIN-FENG CHIANG, CHENG-EN HSU and TSE-CHING YANG

Iron & Steel Research & Development
China Steel Corporation

Steel and steel-reinforced concrete structures are widely employed in ultra-high-rise and large-span buildings. Currently, to improve fabrication efficiency, electroslag welding (ESW), with high deposition rate has been adopted for filling the T-joint between skin and diaphragm plates, replacing flux core arc welding in box-column production. However, ESW with high heat input would significantly reduce the impact toughness of the weld joints, including both the weld metal and heat-affected zone (HAZ). This investigation elucidates the effect of the titanium-to-nitrogen (Ti/N) ratio on the impact toughness improvement of the electroslag weld joints in CSC 60 kgf/mm²-grade steel plates. The Charpy V-notch specimens were extracted from the as-welded T-joints produced with the heat input in the range between 704 and 849 kJ/cm. The results indicate that reducing the Ti/N ratio from 4.06 to 2.89 increases the Charpy V-notch impact toughness at -5 ˚C from 51 J to 138 J at the fusion line and from 61 J to 143 J in the coarse-grained HAZ, respectively. This improvement is attributed to the higher density of inclusions, resulting in a finer microstructure. These findings provide valuable insights for optimizing steel composition and welding parameters in high-performance structural applications.

Keywords: Box column, Structural steel, Electroslag welding, Impact toughness, Ti/N ratio

1. INTRODUCTION

Box columns are essential load-bearing members in both steel and steel-reinforced concrete structures. They are generally fabricated by assembling vertical skin plates with horizontal diaphragm plates. To improve manufacturing efficiency, electroslag welding (ESW), characterized by a high deposition rate and considerable heat input, is commonly employed to fill the pre-gapped joints between the skin and diaphragm plates. Subsequently, submerged arc welding is performed to fill the grooved corners of the column to ensure structural integrity[(1)].

Due to the high heat input of the ESW process, the cooling rate during solidification is relatively slow, often resulting in the formation of coarse grains or brittle phases. These microstructural changes may significantly deteriorate the crack resistance of the welded joint. Hence, in addition to selecting proper consumables, the use of base steel plates with high impact toughness is critical for ensuring weld performance.

Recent studies have demonstrated that the titanium-to-nitrogen (Ti/N) ratio in low-carbon steels plays a key role in controlling microstructure and enhancing low-temperature toughness. Liu et al. investigated the effect of Ti/N ratios (5.85, 4.22, and 2.82) in 0.08 wt.% C steels and reported that the steel with the lowest Ti/N ratio exhibited the highest impact toughness at -20°C, attributed to its most refined microstructure[(2)]. Similarly, Zhang et al. compared Ti/N ratios of 3.0 and 5.7 under identical cooling conditions and found that lower Ti/N ratios led to refined inclusions and restricted migration of prior austenite grain boundaries, thereby improving toughness[(3)].

While numerous studies have addressed the influence of Ti/N ratio on impact performance, most have been based on thermal simulations using the Gleeble system, which may not fully replicate the thermal cycles encountered during actual welding. Therefore, the transferability of these findings to real fabrication remains limited. In this study, the impact toughness and microstructural evolution of low-carbon steel plates with varying Ti/N ratios are evaluated under realistic ESW conditions. The entire T-joint section within the box-column assembly, including skin plates, diaphragm plates, and backing plates, undergoes the complete thermal cycle of the ESW process, providing a more representative assessment of structural performance.

2. EXPERIMENTAL METHOD

2.1 Materials

Two 60 kgf/mm²-grade structural steel plates with different Ti/N ratios were used in this study. The first plate had a Ti/N ratio of 4.06, denoted as HTN, while the second plate had a Ti/N ratio of 2.89, denoted as LTN. Both plates were 75 mm thick. These plates were assembled with 50 mm-thick diaphragm plates and 40 mm-thick backing plates, both possessing a Ti/N ratio of 3.33, to form T-joint specimens for the ESW process.

In order to evaluate tensile strength, additional beam plates (50 mm thick) with the same chemical composition as the diaphragm and backing plates were also welded to the T-joint specimens. A high-strength consumable wire (60 kgf/mm² grade) was used as the filler metal.

2.2 Welding process

ESW was performed to fill a 600 mm-long gap using a Lincoln® ESW welding machine. The welding current and voltage were performed in the range between 380 and 400 A, and 50 and 52 V, respectively. The welding velocities were 1.47 mm/min for the HTN condition and 1.62 mm/min for the LTN condition, respectively, which is sensitive on the instantaneous deposition rate. Based on these parameters, the calculated heat input ranged from 766 to 839 kJ/cm for HTN and from 704 to 770 kJ/cm for LTN, with similar overall heat input between the two conditions.

To produce tensile test specimens, a beam plate was welded to each T-joint using gas metal arc welding (GMAW) with the same high-strength filler wire. The GMAW process was carried out with a welding current of 270–280 A, welding voltage of 27–28 V, and a travel speed of 300 mm/min. The calculated heat input of GMAW ranged from 14.6 to 15.7 kJ/cm, was much lower than that of ESW.

2.3 Material characterization

As-welded specimens were sectioned perpendicular to the weld direction and prepared for microstructural observation and Vickers hardness testing. The cross-sectional surfaces were ground, polished, and etched with a 5 vol.% nital solution to reveal the weld microstructure.

Charpy V-notch (CVN) impact tests were conducted in accordance with ASTM E23. Notches were positioned at three distinct locations: on the fusion line (FL), 1 mm into the weld metal (FL–1), and 1 mm into the heat-affected zone (HAZ) (FL+1). All impact tests were performed at –5°C using specimens pre-cooled in alcohol at the same temperature, following the JASS 6 standards from the Architectural Institute of Japan.

Microstructural observations were conducted using an optical microscope (Vario, Carl Zeiss). Vickers hardness testing was carried out along a line from the diaphragm through the weld metal to the skin plate using a Duramin-100 hardness tester (Struers) with a load of 10 kgf and an interval of 1 mm.

3. RESULTS AND DISCUSSIONS

3.1 Microstructure and Hardness

Figure 1 shows the overall morphology of the ESW and GMAW joints for both HTN and LTN conditions, along with their corresponding Vickers hardness distributions. The single-pass weld metal (WM) produced by

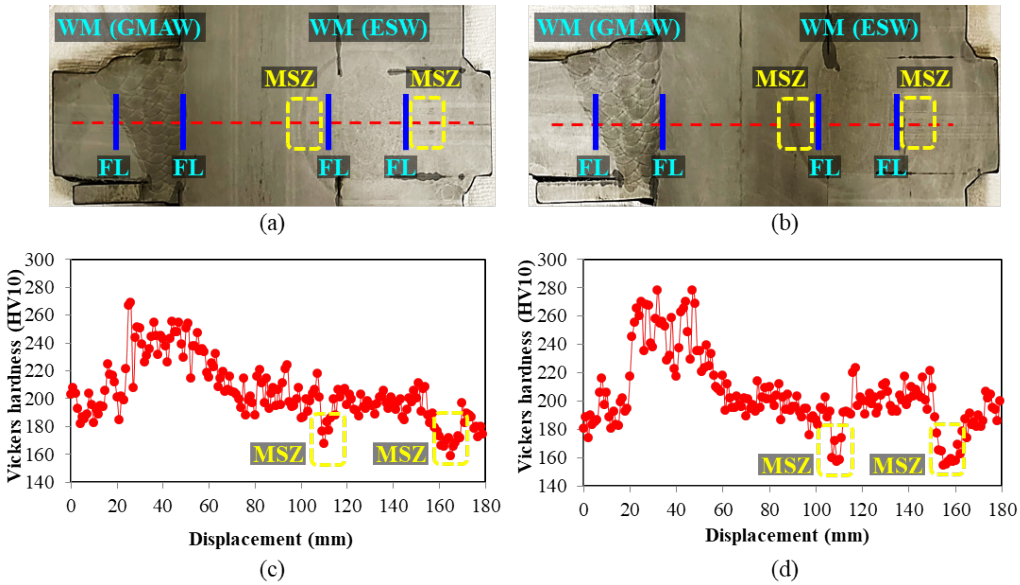

Fig.1. The macrograph of (a) HTN and (b), as well as the hardness distribution for (c) HTN and (d) LTN.

ESW and the multi-pass WMs created by GMAW are presented in Figure 1(a) and 1(b), respectively. The hardness testing was conducted at mid-thickness along the beam, skin, and diaphragm plates, as shown in Figures 1(c) and 1(d).

Both HTN and LTN conditions exhibited similar hardness values in the ESW weld metal, ranging from 180 to 210 HV. The dominant microstructures observed in these welds were grain boundary ferrite (GBF) and acicular ferrite (AF), as shown in Figure 2. The noticeable softening zones with hardness between 160 HV and 180 HV were also identified surrounding the ESW weld metals, referred to as the most softened zone (MSZ). This is attributed to the thermal cycle of ESW, particularly where the peak temperature lies between Ac_1 and Ac_3, leading to a phase transformation in the $\alpha + \gamma$ region. The slow cooling rate further promotes the formation of coarse polygonal ferrite (PF) and pearlite (P), as shown in Figure 3(a) and 3(c) for HTN and LTN, respectively. In contrast, the base metal (BM) areas of the skin plates (Figure 3(b) and 3(d)) maintained finer microstructures. In comparison, no distinct softening

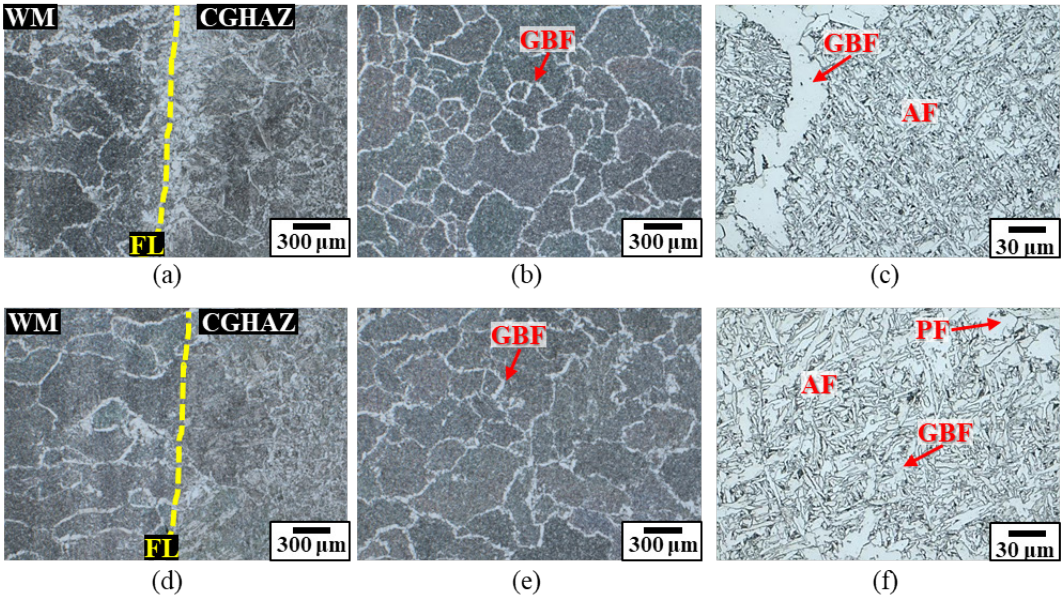

Fig.2. The microstructure at (a) FL, (b) WM, and (c) WM with high-magnified view in HTN, as well as (d) FL, (e) WM, and (f) WM with high-magnified view in LTN.

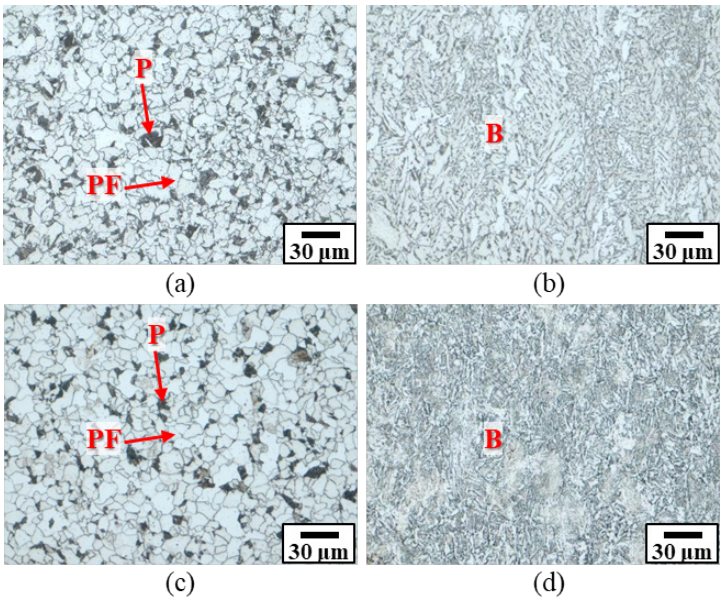

Fig.3. The microstructures of the (a) MSZ and (b) BM in HTN, as well as the (c) MSZ and (d) BM in LTN.

zone was observed in the GMAW regions due to its significantly lower heat input compared to ESW.

3.2 Mechanical properties

Figure 4 shows the Charpy impact toughness results at -5°C for both HTN and LTN specimens, as can be seen, all the results greater than 27 J satisfy the toughness requirement. In addition, the impact energies at the FL–1 positions are similar between both conditions, but the energies in the HTN condition at the FL and FL+1 positions are clearly lower than those in the LTN condition.

Tensile stress–strain curves for HTN and LTN are shown in Figure 5, with values of 574, 579, and 577 MPa for the three HTN tests, and 578, 586, and 582 MPa for the LTN tests. All of them satisfied the minimum tensile strength requirement for 60 kgf/mm²-grade structural steel (570 MPa). The fracture occurred exclusively at the MSZ within the diaphragm, as illustrated in Figure 6, consistent with the location of the lowest hardness and smallest cross-sectional area perpendicular to the loading axis.

3.3 Effect of Ti/N ratio on the impact toughness

Although no significant difference was observed in tensile strength between HTN and LTN, the LTN specimens consistently exhibited higher impact toughness at both FL and FL+1 positions. This improvement is primarily attributed to microstructural changes in the heat-affected zone (HAZ). The lower Ti/N ratio in the LTN steel promoted a higher density of dispersed particles in the molten pool. These inclusions act as effective pinning sites for grain boundary migration, facilitating the formation of a finer microstructure during cooling, which is also reported in previous studies[2, 4].

Additionally, GBF grains in LTN were not continuously aligned along prior austenite grain (PAG) boundaries, which further enhances toughness[2, 5]. Since cracks often initiate at the fusion line and propagate into either the WM or HAZ, improving the toughness in both regions contributes significantly to the overall crack resistance of the FL position.

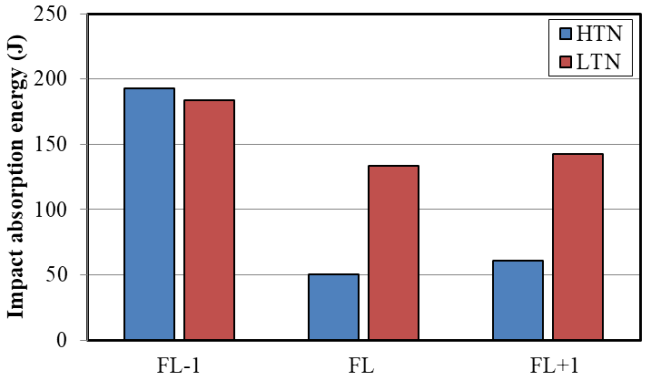

Fig.4. Charpy impact energy at –5 °C of HTN and LTN conditions at FL–1, FL, and FL+1 positions.

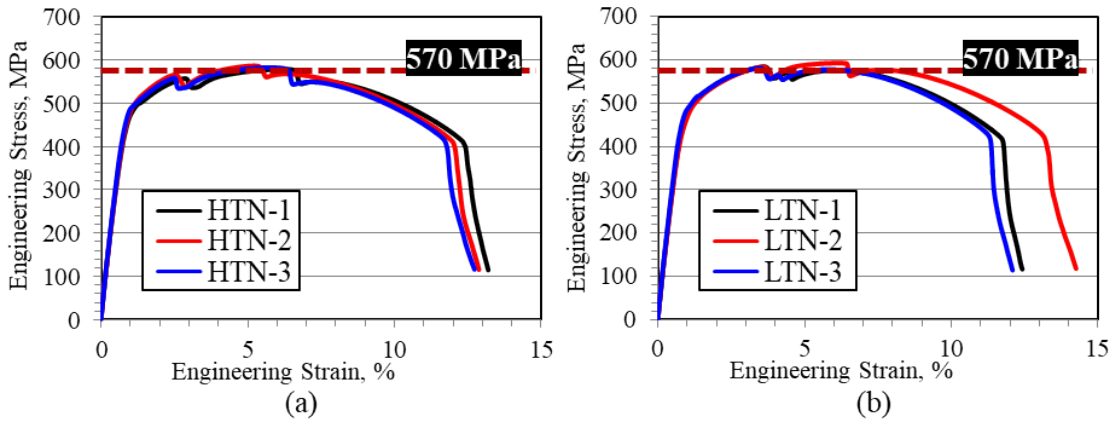

Fig.5. Tensile stress–strain curves of (a) HTN and (b) LTN.

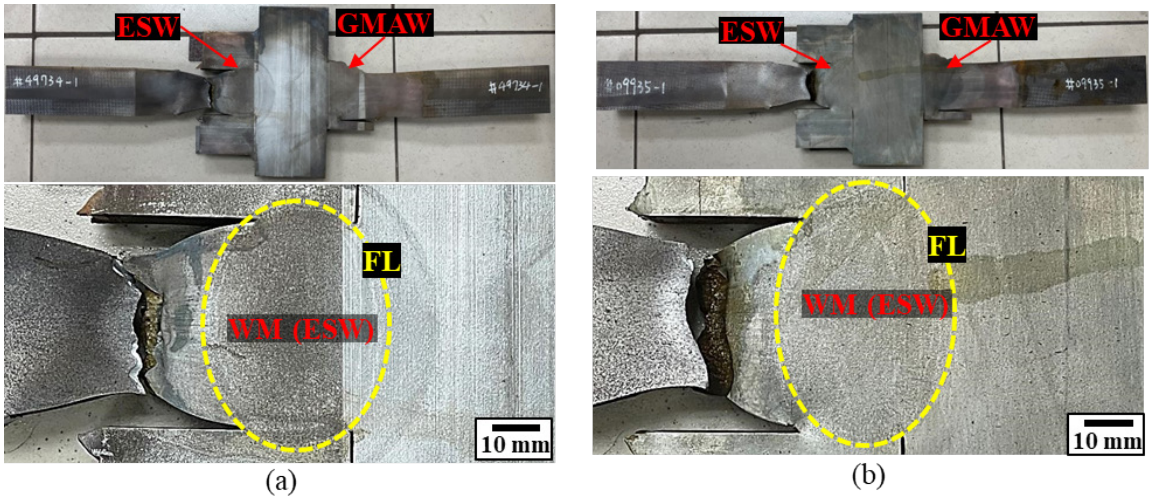

Fig.6. Fractured tensile specimens of (a) HTN and (b) LTN.

This study clearly demonstrates the influence of Ti/N ratio on the impact toughness of ESW-fabricated T-joints and provides insight into the underlying metallurgical mechanisms.

4. CONCLUSIONS

This study investigated the effect of Ti/N ratio on the impact toughness of structural steel subjected to high heat input ESW. Based on the experimental results, the following conclusions can be drawn:

(1) Both HTN and LTN conditions exhibited tensile strengths above 570 MPa after ESW, satisfying the minimum strength requirement for 60 kgf/mm²-grade structural steel.

(2) The impact toughness values at -5°C were similar at the FL–1 position for both HTN and LTN. This is attributed to the similar dilution effect from the consumable filler, skin plate, diaphragm, and backing plates, despite the slight differences in chemical composition between HTN and LTN skin plates.

(3) The impact toughness at the FL and FL+1 was significantly improved in the LTN condition. This improvement is primarily due to microstructural refinement in the HAZ, promoted by a higher inclusion density resulting from the lower Ti/N ratio.

REFERENCES

1. A. Kojima, R. Uemori, M. Hoshino, K. Ishida, A. Kiyose, M. Minagawa, T. Nakashima, H. Yasui, “Super High HAZ Toughness with Fine Microstructure Imparted by Fine Particles,” NIPPON STEEL TECHNICAL REPORT, No. 90 (2004) pp. 2-6.
2. J. Liu, J. Wang, F. Hu, K. Fu, Z. Zhang, Y. Wu, “Effects of Ti/N Ratio on Coarse-Grain Heat-Affected Zone Microstructure Evolution and Low-Temperature Impact Toughness of High Heat Input Welding Steel,” Coatings, 13 (2023) 1347.
3. Y. Zhang, Y. Zhang, J. Yang, T. Li, Y. Chen, “Influence of Ti/N Ratio on Inclusions Microstructures and Toughness in Heat-Affected Zone of Shipbuilding Steel Plates with Mg Deoxidation after High Heat Input Welding,” Steel Research International, 2023.
4. T. Koseki, G. Thewlis, “Overview Inclusion assisted Microstructure Control in C Mn and Low Alloy Steel Welds,” Materials Science and Technology, 21 (2005) pp. 867-879.
5. J.P. Wang, Z.G. Yang, B.Z. Bai, H.S. Fang, “Grain Refinement and Microstructural Evolution of Grain Boundary Allotriomorphic Ferrite Granular Bainite Steel After Prior Austenite Deformation,” Materials Science and Engineering A, 369 (2004) pp. 112-118.